

**FA2-MS16-P10**

**Crystal Chemistry of SnX-PbX (X=S, Se) mixed crystals.** Sandra Lobe<sup>a</sup>, Klaus Bente<sup>a</sup>, Sven Gerhardt<sup>a</sup>, Martin Gampe<sup>a</sup>, Christian Koppka<sup>a</sup>, Daniel Schrader<sup>a</sup>  
<sup>a</sup>*Institut für Mineralogie, Kristallographie und Materialwissenschaft, University of Leipzig.*  
 E-mail: [sandra.lobe@uni-leipzig.de](mailto:sandra.lobe@uni-leipzig.de)

The systems SnS-(Pb,Sn)S; SnS<sub>0.75</sub>Se<sub>0.25</sub>-(Pb,Sn)S<sub>0.75</sub>Se<sub>0.25</sub>, SnS<sub>0.5</sub>Se<sub>0.5</sub>-(Pb,Sn)S<sub>0.5</sub>Se<sub>0.5</sub> and SnS<sub>0.25</sub>Se<sub>0.75</sub>-(Pb,Sn)S<sub>0.25</sub>Se<sub>0.75</sub> were investigated to determine the regions where solid solutions exist. There the crystals have orthorhombic structure. The miscibility gaps have been determined by electron microprobe analysis and X-ray powder diffraction. The samples were synthesized by solid state reaction in closed silica ampoules. The width of solid solution range, i.e. the Pb/Sn-ratio too, depends strongly on the S/Se-ratio. The lattice parameters of the orthorhombic phases were determined by X-ray powder diffraction. To grow single crystals via chemical vapour transport this powder was used as source material. Iodine acts as transporting agent. These single crystals should have a good electrical conductivity similar to SnS-(Pb,Sn)S films grown by vacuum evaporation [1].

[1] K. Bente, V. V. Lazenka, D. M. Unuchak, G. Wagner, and V. F. Gremenok, Cryst. Res. Technol. 45, No. 6, 643 – 646 (2010) / DOI 10.1002

**Keywords:** semiconductor, sulfosalts, lattice parameters

**FA2-MS16-P11**

**Dense packing of identical ellipses with 6 contacting neighbours.** Takeo Matsumoto<sup>a,b</sup>, Masaharu Tanemura<sup>c</sup>.  
<sup>a</sup>*Kanazawa University, Kanazawa, Japan*, <sup>b</sup>*National Inst. Advanced Industrial Science and Technology, Tsukuba*. <sup>c</sup>*Inst. of Statistical Mathematics, Tokyo, Japan*.  
 E-mail: [matsumoto.ty.920@biscuit.ocn.ne.jp](mailto:matsumoto.ty.920@biscuit.ocn.ne.jp)

For the densest packings of ellipsoids and ellipses, Matsumoto and Nowacki first discussed and derived 13 and 2 different densest packings of ellipsoids and ellipses respectively [1]. They assumed that the densest packings are only those which result from the closest packings of spheres (ccp and hcp) and circles by an affine transformation respectively. The packing density and the contact number of these packings for ellipsoids are  $\rho = \pi/3\sqrt{2} = 0.74048\dots$ , and  $N=12$ , the same as the ccp or hcp. And the density of derived packings of ellipses is  $\rho = \pi/2\sqrt{3} = 0.906899\dots$ , and the contact number is  $N=6$ . Moreover, they are all homogeneous packings, namely all ellipsoids or ellipses, are crystallographically equivalent. There are 7 dense homogeneous packings of ellipses with 6 contacting neighbours [2],[3]. Among them, 2 types of  $p2$  and  $c2mm$  attain the maximum density, 0.906899 being the same of the closest packing of circles,  $p6mm$  [1]. The  $p2gg-2a2$  packing cannot attain the maximum density [4]. Since 1992, Tanemura and Matsumoto have presented the proof, with the aid of computer, that the other 3 types of packings of ellipses,  $p31m$ ,  $p3$ , and  $p2gg-4c1(I)$ , cannot exceed the maximum density of circles [5],[6] and [7]. The packing density depends on axial ratio  $k=a/b$  for  $p31m$ , and a tilt angle  $\theta$  of major axis together with the shape parameter  $k=a/b$  for  $p3$ , and  $p2gg-4c1(I)$ . The other  $p2gg-4c1(II)$  packing of ellipses also shows no maximum density and is composed of

$p2$  and  $p2gg-2a2$  regions. The packing density is the function of the shape parameter  $k=a/b$  and the tilting angle  $\theta$  [8],[9]. Concerning the dense packings of ellipsoids and ellipses, superdense crystal packings of ellipsoids have been reported [10]. Even though we cannot understand these packings, the contradict packings of ellipses with the hypothesis in [1], are not found.

[1] Matsumoto, T., Nowacki, W., *Zeit.Krist.*1966, 23,6,401-421. [2] Nowacki,W.,*Schweiz.Mineral.Petrog.Mitt.*1948, 28,502. [3] Grünbaum,B., Shephard,G.C., *Tilings and Patterns, Freeman*,1987. [4] Matsumoto,T., *Zeit.Krist.* 1968, 126, 170-174. [5], [6],[7] Tanemura, M., Matsumoto, T., *Zeit.Krist.*, 1992, 198, 89-99. 1995., 210, 585-596. 1997, 212,637-647. [8] Matsumoto,T., Tanemura,M., *Ecm24*, 2007,*Abst.* MS45,P01,s282. [9] Tanemura,M., Matsumoto,T., in preparation. [10] Donev, A., Stillinger,F.A., Chaikin,P.M.,Torquato,S., *Arxiv:cond-mat/0403286 v1 10 Mar.2004*.

**Keywords:** packings of ellipses and ellipsoids; dense packings; homogeneous packings

**FA2-MS16-P12**

**Structure and Energetics of the FeOOH Polymorphs and their Surfaces from First Principles.** Katrin Otte, Rossitza Pentcheva, Wolfgang W. Schmahl. *Section Crystallography, Department of Earth and Environmental Sciences, University of Munich, Germany.*  
 E-mail: [katrin.otte@lrz.uni-muenchen.de](mailto:katrin.otte@lrz.uni-muenchen.de)

Iron oxyhydroxides (FeOOH) play an important role in a series of environmental and technological processes, e.g. in binding heavy metals. Using density functional theory (DFT), we study the bulk properties of the FeOOH polymorphs goethite ( $\square$ ), akaganeite ( $\square$ ), lepidocrocite ( $\square$ ), and the high pressure phase ( $\square$ ) at ambient conditions and under hydrostatic pressure. The energetic relations among the phases reveal that the framework structure ( $\square$ ) are more favorable than the layered one ( $\square$ ) [1]. Moreover, we explore the stabilization of akaganeite by filling the large 2x2 channels with ions such as  $\text{Cl}^-$ ,  $\text{SO}_4^{2-}$  or  $\text{AsO}_4^{3-}$ . The FeOOH polymorphs have high surface areas and high adsorption affinities for aqueous solutes [2]. Therefore, we analyze structural, energetic, and sorption properties of the bare and hydroxylated goethite(101), akaganeite(100), and lepidocrocite(010) surfaces.

We acknowledge funding through the BMBF Geotechnologies Program “Mineral Surfaces” and a grant for computational time at the Leibniz Rechenzentrum.

[1] K. Otte, R. Pentcheva, W. W. Schmahl, and J. R. Rustad, Phys. Rev. B 80, 205116 (2009). [2] R. M. Cornell and U. Schwertmann, *The Iron Oxides* (Wiley, Weinheim, 2001).

**Keywords:** FeOOH, sorption, DFT

**FA2-MS16-P13**

**Crystal structure solution of the mineral sanjuanite from laboratory powder diffraction data.** Colombo, F.<sup>a</sup>, Rius, J.<sup>b</sup>, Panunzio, E.V.<sup>c</sup>.  
<sup>a</sup>*Cátedra de Geología General, Universidad Nacional de Córdoba, Argentina*, <sup>b</sup>*Institut de Ciència de Materials de Barcelona (CSIC), 08193 Bellaterra, Catalonia, Spain*, <sup>c</sup>*Instituto de Físico-Química, Universidad Nacional de Córdoba, Argentina*.

E-mail: [jordi.rius@icmab.es](mailto:jordi.rius@icmab.es)

Sanjuanite,  $\text{Al}_2(\text{PO}_4)(\text{SO}_4)\text{OH}\cdot 9\text{H}_2\text{O}$ , is a fibrous mineral found in Carboniferous slates at the Pocito Department, San Juan province, Argentina. This phase was first described in [1] and is chemically related to other hydrated aluminium phosphate-sulphate minerals like kribergite  $\text{Al}_5(\text{PO}_4)_3(\text{SO}_4)(\text{OH})_4\cdot 2\text{H}_2\text{O}$  [2] and hotsonite  $\text{Al}_{11}(\text{PO}_4)_2(\text{SO}_4)_3(\text{OH})_{21}\cdot 16\text{H}_2\text{O}$  [3]. Unfortunately, the structural relationship among these minerals is difficult to establish, since no specimens suitable for single-crystal experiments are available, and no isostructural materials are known. To increase the knowledge on these compounds, the crystal structure of sanjuanite was solved and refined from intensity data collected on a conventional powder diffractometer (Bragg-Brentano geometry, scintillation detector, secondary graphite monochromator,  $\text{CuK}\alpha_{1,2}$  radiation). The first necessary step was the indexing of the powder pattern. Unlike the triclinic unit cell previously proposed in [4], the new monoclinic cell  $a=14.3719(3)$ ,  $b=17.2381(4)$ ,  $c=6.1110(2)$  Å,  $\beta=106.617(21)^\circ$ ,  $V\cong 1452$  Å<sup>3</sup> indexes all reflections and hence was used for extracting the integrated intensities down to a  $d$ -spacing of 1.30 Å. This data set was further processed with S-FFT based direct methods [5]. With the exception of one O atom, all non-H atoms clearly showed up in the Fourier synthesis computed with the refined phases from the best direct methods solution. Once the crystal structure model was completed, it was optimized by restrained Rietveld refinements to an effective  $\chi^2$  value of 2.08 [6]. During the refinement the slight preferred orientation along  $[-2\ 0\ 3]$  detected in the flat sample was treated with the March-Dollase correction. The structure of sanjuanite (space group  $P2_1/a$ ,  $Z=4$ ) is composed of infinite alumino-phosphate chains running parallel to  $c$ . Isolated  $(\text{SO}_4)^{2-}$  groups and  $\text{H}_2\text{O}$  molecules connect the groups of chains. Hydrogen bonding plays a key role in the stabilization of the structure.

[1] De Abeledo, M.E.J.; Angelelli, V.; De Benyacar, M.A.R.; Gordillo, C., *Amer. Mineral.*, 1968, 53,1. [2] DuRietz, T; *Geol.För Förh.*, 1945, 67, 78. [3] Beukes, G.J.; Schoch, A.E., Van der Westhuizen, W.A.; Bok, L.D.C.; De Bruijn, H.; *Amer. Mineral.*, 1984, 69,979. [4] De Bruijn, H.; Beukes, G.J.; Van der Westhuizen, W.A.; Tordiffe, E.A.W., *Mineral.Mag.*, 1989, 53, 385. [5] Rius, J.; Frontera, C., *J. Appl. Cryst.*, 2007, 40, 1035. [6] Rius, J.; (2008) *RIBOLS, A Fortran program for Rietveld refinement*, Institut de Ciència de Materials de Barcelona (CSIC).

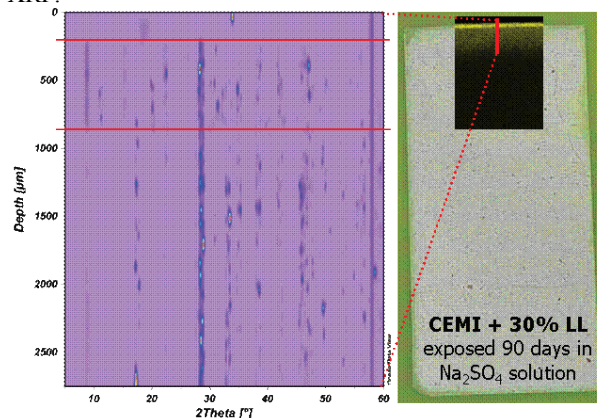
**Keywords:** sanjuanite, ab-initio solution, powder diffraction

#### FA2-MS16-P14

**High resolution phase analyses and early crystallization processes of cement.** Moritz-C. Schlegel<sup>a</sup>, Urs Mueller<sup>a</sup>, Ulrich Panne<sup>a</sup>, Franziska Emmerling<sup>a</sup>. <sup>a</sup>BAM Federal Institute of Materials Research and Testing, Berlin, Germany *Materials Science, Technical University Darmstadt, Germany*. E-mail: [moritz-caspar.schlegel@bam.de](mailto:moritz-caspar.schlegel@bam.de)

Cementitious building materials are a substantial part of our built environment. Due to the nature of the cementitious binder those materials can be described as multi component nano composite materials. Furthermore, for studying degradation mechanisms spatial chemical or phase analytical data are needed, which can be linked to the microstructure of the cementitious paste. The objectives of this work are the

observation of the early crystallization of cement during the hydration and the analysis of the phase assemblage of chemical attacked mortar and concrete including synchrotron methods. Both objectives were examined by diffraction with synchrotron radiation in transmission geometry ( $\lambda=1.0656$  Å,  $\mu$ -spot beamline, BESSY II, HZB, Berlin). The latter one is performed using an ultrasonic trap. That was provided the contact free analysis of a sample and ensures a constant water cement ratio. This is a tremendous improvement since former studies using capillaries coupled with water injection system could not guarantee a homogeneous dispersion of water within the cement suspension. The integration time for a single diffraction pattern was about 30 sec and allowed a detailed view into the dynamics of the crystallization processes at early stages. The spatial phase analysis was performed on cement paste and mortar specimens, which were exposed to sulphate and chloride solutions. The reaction fronts of sulphur and chloride were localised by elemental mapping with a micro X-ray fluorescence analysis. Synchrotron X-ray diffraction was used in-situ for the identification of the phase composition (Fig. 1). The primary focussing optics established a spatial resolution of 10  $\mu\text{m}$  for thick section samples with a thickness of ca. 200  $\mu\text{m}$ . That means phase analysis can be performed in-situ with a high local resolution and within the intact micro structure of the sample. First results show patterns with a good peak to background ratio. The measurement of sulphate content exposed cement paste samples reveal a phase composition, determined by synchrotron XRD which corresponds well to the chemical profile measured by micro XRF.



**Keywords:** cement, time-resolved, space-resolved

#### FA2-MS16-P15

**Elastic anomalies and electromechanical properties of tourmalines.** Chandra Shekhar Pandey, Jürgen Schreuer. *Institut für Geologie, Mineralogie und Geophysik, Ruhr-Universität Bochum, Germany*. E-mail: [schreuer@ruhr-uni-bochum.de](mailto:schreuer@ruhr-uni-bochum.de)

Tourmalines exhibit a broad variability in chemical composition and are a promising piezoelectric material for acoustic-electronic devices operating at high-temperatures. In contrast to  $\alpha$ -quartz,  $\text{LiNbO}_3$  and materials of the langasite family, the application of tourmaline at temperatures up to its melting point is not limited by phase transitions, electrical conductivity or strong ultrasound dissipation effects.

Here we report the full set of elastic and piezoelectric constants of five natural single crystal tourmalines of gem quality between room temperature and 903 K as determined